



The future of failure: stress or strain?

Juan Watterson

Fault Analysis Group, Liverpool University Marine Laboratory, Port Erin, Isle of Man, IM9 6AJ, British Isles

Received 6 April 1998; accepted 5 November 1998

Abstract

Strains in rocks can be observed but ancient stresses can only be inferred. We should re-examine the potential of strain geometry as the key to understanding and interpreting common shear structures ranging from faults to plastic shear zones. The concept of failure along zero extension directions can be applied to natural structures in rocks and is predicated on strain compatibility between differently strained volumes. Zero extension directions are considered for two strain configurations, plane strain ($k = 1$) and uniaxial shortening ($k = 0$). The crucial difference between shear fractures, or faults, and plastic yield zones is that the former are preceded by dilatation while the latter are isovolumetric. Volume changes during deformation affect the orientations of zero extension directions and hence of the resulting structures. With isovolumetric strain, yield occurs on planes at 45° to the principal shortening direction in plane strain and at 54.7° to this axis in uniaxial shortening. Uniaxial shortening experiments on rock samples allow estimation of the relative volumetric strains when yield zones initiate. When this volumetric strain is used to estimate the orientation of shear fractures in plane strain, ca 70° dips are predicted for normal faults at high crustal levels, decreasing downwards to 45° . © 1999 Elsevier Science Ltd. All rights reserved.

1. Introduction

Because we deal with relatively large, and therefore observable, strains, geologists generally have a much better understanding and appreciation of strains and displacements than we have of stresses and forces, which in any case can only be speculative for ancient events. Vindication of this cultural predisposition is provided by Burland (1965), (quoted in Roscoe, 1970), who pointed out that while “stress is a philosophical concept—deformation is a physical reality”. Engineers often express problems in terms of stress partly because most engineering materials undergo very little strain before disruptive failure and partly because stresses and forces acting on engineered systems can be either calculated or measured, albeit indirectly. But engineering practice provides no basis for geologists either to view stress as a ‘cause’ of deformation (Edelman, 1989) or for a conjectural stress configuration to be the structural geologist’s apotheosis.

In spite of geologists’ familiarity with strain, their

analyses of faulting and of fault systems are very often expressed in terms of stress even though macroscopically ductile shear zones, which form a continuum with faults, are invariably described in terms of strain. This difference in approach determines not only how things are described but, more fundamentally, what questions are asked. The questions asked about faults have traditionally concerned their orientations relative to principal stress axes, with responses invoking Mohr–Coulomb or similar failure criteria based on consideration of stress. The questions asked about shear zones have concerned geometry, strain and displacement. While no single approach is likely to be the one true path to enlightenment, a unified model for the various types of geological shear structures would be helpful. This article attempts to introduce a very preliminary version of a unified strain model for geological heterogeneous yield structures, and is limited to consideration of simple shear structures although the method is also applicable to pure shear structures, e.g. boudins. The immediate question addressed concerns the orientations of simple shear structures, but if the approach is valid it also has potential for development

E-mail address: fault@fag.esc.liv.ac.uk (J. Watterson)

of a model in which yield structures are treated as minimum energy responses to a bulk deformation. The concepts used are well established in those disparate parts of the spectrum of engineering concerned with the properties and behaviours of materials varying from polymers, soils and metals to granular aggregates, and the literature on these topics is drawn on freely. As befits a unified approach, the terms failure and yield are treated as synonyms. 'Plastic' is used in its general sense of deformation by intracrystalline or diffusive flow (Rutter, 1986), encompassing the mechanisms associated with 'macroscopically ductile' shear zones.

My interest in the topic arose from field work on conjugate sets of syn-kinematic mafic dyke swarms and on related strike-slip shear zones (Watterson, 1978). For both, conjugate angles containing the shortening direction are $>90^\circ$, giving rise to the obvious question—why obtuse angles?

2. Constant volume strain

2.1. Orientations of shear zones and faults

A critical difference between plastic shear zones on the one hand and 'brittle' faults on the other, is that the conjugate angle containing the principal shortening axis of the bulk strain is $\geq 90^\circ$ in the case of shear zones and is $< 90^\circ$ for faults (Ramsay and Huber, 1987, p. 612), typically $40\text{--}60^\circ$ for normal faults (Anderson, 1951). Another crucial difference between plastic yield and brittle failure in rocks is that the former is generally, although not necessarily, a constant volume process whereas the latter is always associated with a dilatation, or positive volume strain (Rutter, 1986). This difference suggests that the controls on orientations of plastic shear zones might be more simply defined than those of faults, which represent a non-isovolumetric variation of the less complex isovolumetric case. Following this line of argument we first examine the controls on orientations of plastic shear zones. It is argued that localised shear failure takes place parallel to zero extension directions in the matrix. Discussion is limited to the two bulk strain, or loading, configurations represented by plane strain and by uniaxial shortening, with discussion of the isovolumetric case followed by that of the non-isovolumetric case.

2.2. Plastic shear zones

The simplest case to consider is that of localised simple shear zones accommodating a bulk pure shear plane strain, with no volume strain. The bulk deformation is assumed to be accommodated exclusively on

numerous shear structures each of which is small relative to the strained volume, so neither the boundaries nor the shape of the volume play a significant role in determining either the locations, orientations or geometries of the localised strains. The bulk strain is the sum of the high local strains, shear zones, and the lower matrix strains. A major attraction of the simple shear model for rock deformation on both small (Ramsay and Graham, 1970) and large scales (Escher et al., 1975) is that a high strain shear zone remains compatible with its matrix without a discontinuity developing between the two. This compatibility exists because a shear zone boundary is parallel to the plane of shear, within which every direction is a line of no finite longitudinal strain, and is also a line of no infinitesimal longitudinal strain. Ideally, therefore, there is no 'misfit', or strain incompatibility, between either (i) the deformed shear zone and its, supposedly unstrained, matrix, or (ii) regions of different shear strain magnitudes within the shear zone, so long as the shear strain contours are parallel to the shear zone boundary, or shear plane. Any strain gradient within a shear zone can be accommodated compatibly so long as the gradient is normal to the shear plane. Strictly speaking, strain compatibility requires only that longitudinal strains on either side of a shear zone boundary are the same rather than zero but, in practice, non-zero identical strains would represent a very special case (Treagus, 1983) not likely to occur with a simple shear zone. Complications do arise nevertheless, because strain gradients parallel to the shear plane must occur in order to accommodate the lateral displacement gradients which are universally present along both shear zones and faults. These complications are not considered further as they do not affect the conclusions. What follows does not conflict with the shear zone model of Ramsay and Graham (1970) but simply extends it by imposing more restrictive conditions.

The now traditional shear zone model predicts nothing explicitly about the orientation of a geological shear zone because, as its matrix is considered as undergoing no strain, all shear zone orientations are equally compatible with their matrix; although if strain is accommodated entirely by shear zones their orientations must be such as to accommodate the imposed bulk strain. The freedom of orientation arises from a simplification in the model, which is that the matrix is considered as being unstrained and therefore not contributing to the bulk strain. In practice, there will always be a penetrative strain of the matrix, either elastic or both elastic and permanent. As is shown below, if the local and matrix strains are compatible, the principal strain axes of the bulk strain will be congruent with those of the matrix strain.

The potential strain incompatibility between a shear zone and its matrix is, therefore, the key factor deter-

mining the most likely orientation of a shear zone. Although strain compatibility is expressed in terms of geometry, the geometry is an implicit proxy for minimum energy as, in principle, all geometries are possible. As compatible strains must be maintained throughout, ideally the problem should be discussed in terms of instantaneous strain rates, or relative strain rates, rather than strains. This is because the strains of concern are those which are taking place at the time when the location and orientation of a shear zone becomes established, which is well before yield occurs. The situation at this instant of time is more precisely represented by strain rates, or relative strain rates, than by accumulated strains. For present purposes this refinement is not necessary so long as it is remembered that all strains referred to are small incremental strains, either elastic or permanent or a combination of the two, which are described by the incremental, or infinitesimal, strain ellipsoid. Only small strains need be considered when we are concerned primarily with the initiation stages of geological shear structures because, for both faults and shear zones, the small initial structures grow into larger displacement structures because of strain softening mechanisms. Although the matrix and bulk strains are here taken to be pure shears, as they are in experimental compression tests, this is only a convenience and there is no intrinsic restriction on the matrix and bulk strain configurations. For brevity, engineering practice is followed by referring to lines and planes of no infinitesimal longitudinal strain as zero extension lines and planes. Local strains (ϵ) have lower case subscripts ($x \geq y \geq z$) and the matrix (and bulk) strains have upper case subscripts ($X \geq Y \geq Z$). Extensional linear strains are taken as positive and are expressed as natural strains (ϵ) where $\epsilon = \ln(1 + e)$, and $e = (l_1 - l_0)/l_0$. For small strains the values of ϵ and e are the same. For an isovolumetric strain, $\epsilon_x + \epsilon_y + \epsilon_z = 0$. Strain ellipsoid symmetries are expressed as values of k , where $k = [Z(X - Y)]/[Y(Y - Z)]$ (Flinn, 1962). Note that a k value is unchanged if there is a component of volumetric strain, because volume change is accommodated by changes in the principal strains accommodating the isovolumetric component of strain.

The conditions to be satisfied when a localised shear zone is formed are that (i) the shear zone must remain coherent with its matrix, and (ii) the local deformation must have its principal strain components in the same ratio to each other as those of the matrix and bulk deformations (Bowden and Jukes, 1972). The requirement for congruent principal strains is self evident when the bulk strain is accommodated only by local strains or only by matrix strains; it is also a requirement when the bulk strain is accommodated by both local and matrix strains, if the matrix and local strains

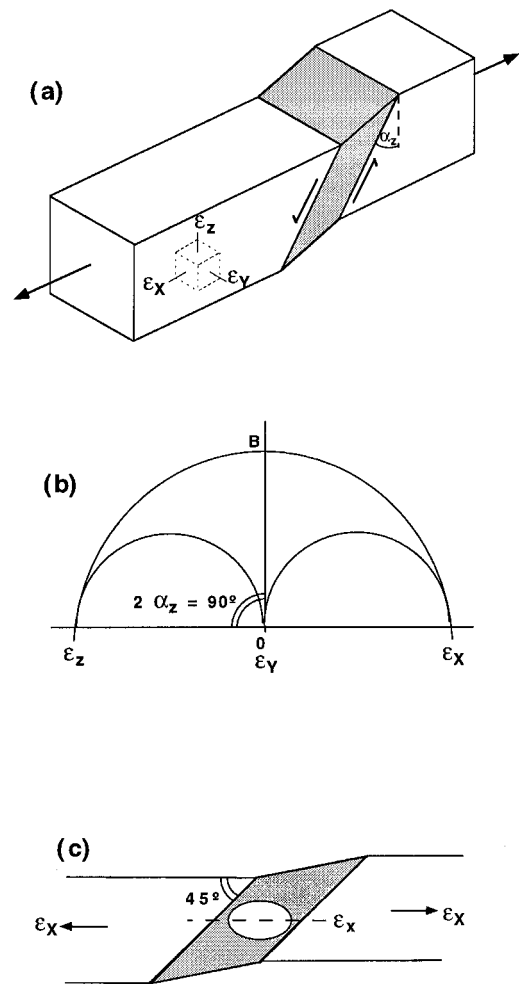


Fig. 1. (a) Schematic representation of simple shear band (stippled) in a volume subjected to plane strain constant volume deformation. Inset cube shows principal axes of matrix and bulk strains. α_z is the angle between the shear band and the Z axis of the bulk strain (after Bowden and Jukes, 1972, fig. 6a). (b) Mohr representation of the matrix and bulk plane strain deformations in (a) showing the locus of the zero extension directions (OB) at 45° to the Z and X axes in the XZ principal plane and parallel to Y in both the XY and YZ principal planes. (c) Section parallel to the XZ principal plane in (a) showing that, as the x axis of the local incremental plane strain ellipsoid lies at 45° to the local shear plane, the local incremental principal extension axis (ϵ_x) is parallel to the X axis of the bulk and matrix strains (ϵ_X). The ellipticity of the principal section of the incremental local strain ellipsoid and the amount of shear are exaggerated.

are not partly to neutralise one other. If both the conditions are to be satisfied then the local deformation can only occur within planar zones which are parallel to planes of zero strain, or zero extension, in both the shear zone and the matrix. In the shear zone the zero extension plane coincides with the shear plane, which therefore should coincide with the zero extension plane

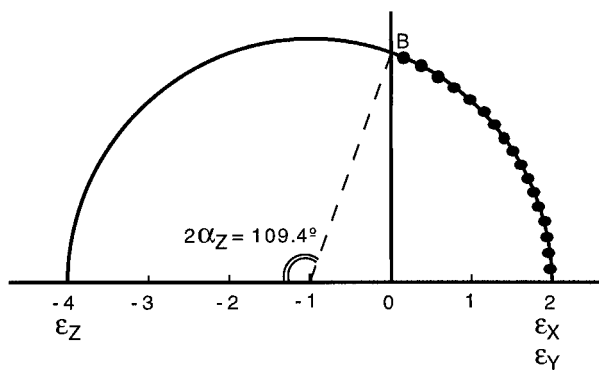


Fig. 2. Mohr circle for isovolumetric $k = 0$ oblate strain, i.e. $\varepsilon_X = \varepsilon_Y = -\varepsilon_Z/2$. All zero extension directions lie at an angle of 54.7° to the Z axis and have a conical locus (OB). Filled circles show the locus of all lines within and parallel to a planar shear band normal to the XZ principal plane and tangential to the conical locus of the zero extension directions. Strain units are arbitrary.

in the matrix, which can be found by using a simple Mohr construction (Fig. 1a and b). As this zero extension plane is a zero extension plane in both the matrix and the shear zone, it is also a zero extension plane of the bulk deformation. In the case of plane strain matrix deformation the zero extension plane lies at an angle of 45° to the maximum (ε_X) and minimum (ε_Z) principal axes of matrix strain (or strain rate), and contains the intermediate principal axis (ε_Y). Fig. 1(c) illustrates the coincidence of the principal strain axes in the local shear zone, in the matrix and in the bulk volume. Only one of the possible two shear zone orientations is shown in Fig. 1 but the orientation of its conjugate pair is evident, either from inspection or by using the complete Mohr circle rather than the abbreviated version shown in Fig. 1(a). For small strains it is evident that the strains in a simple shear zone lying at 45° to the principal extension axis of the bulk strain are parallel to, and therefore compatible with, both the matrix and bulk strains. This conclusion may appear trivial but it illustrates the basis for consideration of shear zone orientations for general matrix strains from $k = 0$ to $k = \infty$ with either positive or negative volume strains. For present purposes it is sufficient to consider only plane strain ($k = 1$) and uniaxial compression ($k = 0$) with, in the first instance, no volume strain.

For a matrix, or bulk, strain where $k \neq 1$ there is no orientation of simple shear zone, i.e. a local strain with $\varepsilon_Y = 0$, which is perfectly compatible with the matrix even for small strains, but the shear zones which do form are those with minimum misfit. As an illustration I take the case of a $k = 0$ bulk deformation, corresponding to a truly oblate strain ellipsoid and to a standard uniaxial compression test. The appropriate Mohr circle is shown in Fig. 2 from which the locus of zero extension directions of the bulk strain is everywhere at 54.7° to the Z axis, i.e. the locus of the zero

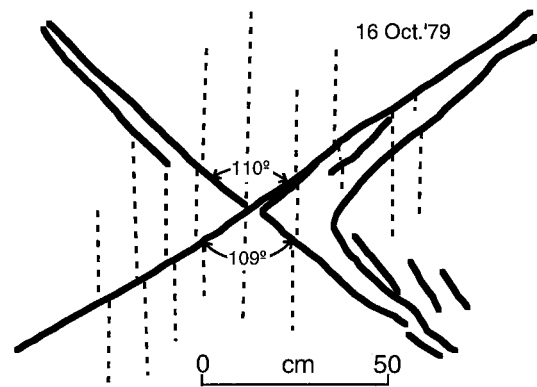


Fig. 3. Yield zones (solid lines) with conjugate angles of 109° and 110° , in sylvinitic roof support pillar at depth of ca 1000 m, Boulby mine, Cleveland, UK. Vertical broken lines represent grooves made by excavator shovel, which are offset along yield zones. From sketch and measurements by Chris Talbot.

extension directions is a conical surface (the 'unstretched cone' of Taylor, 1938), rather than a plane. Clearly, no plane can include more than one zero extension direction of the bulk and matrix strains and the shear zones which form are tangential to the zero extension cone. Any plane tangential to the zero extension cone is a potential shear plane, i.e. any plane which lies at 54.7° to the Z axis. All lines within the shear zone and parallel to the local shear plane are *local* zero extension directions but only one of these, that which is parallel to the local shear direction, is also parallel to a zero extension direction of the bulk and matrix strains. Within the local strain region, strain misfit between a line parallel to the shear plane and a line of the same orientation in the matrix increases with divergence from the shear direction. For example, in a local shear zone which is normal to the XZ principal plane (at 35.3° to X and at 54.7° to Z) the line of greatest misfit is that parallel to Y (see Fig. 2). The X and Y directions are nominal in so far as all strains in the XY plane are equal, so Y is simply at 90° to an arbitrarily defined X axis in the principal plane normal to Z. The locus of all directions within this shear plane is shown by the filled circles on the YZ principal plane in Fig. 2. Representation of the locus of an arbitrary plane in a Mohr construction is described by Treagus (1986).

An alternative view (R. Lisle, personal communication) is that the matrix plane providing least misfit with the zero extension plane of the local strain, is the plane of minimum area change rather than a plane tangent to the zero extension cone. Although the practical differences are slight, this suggestion offers a new line of enquiry.

Examples of conjugate angles of ca 110° bisected by

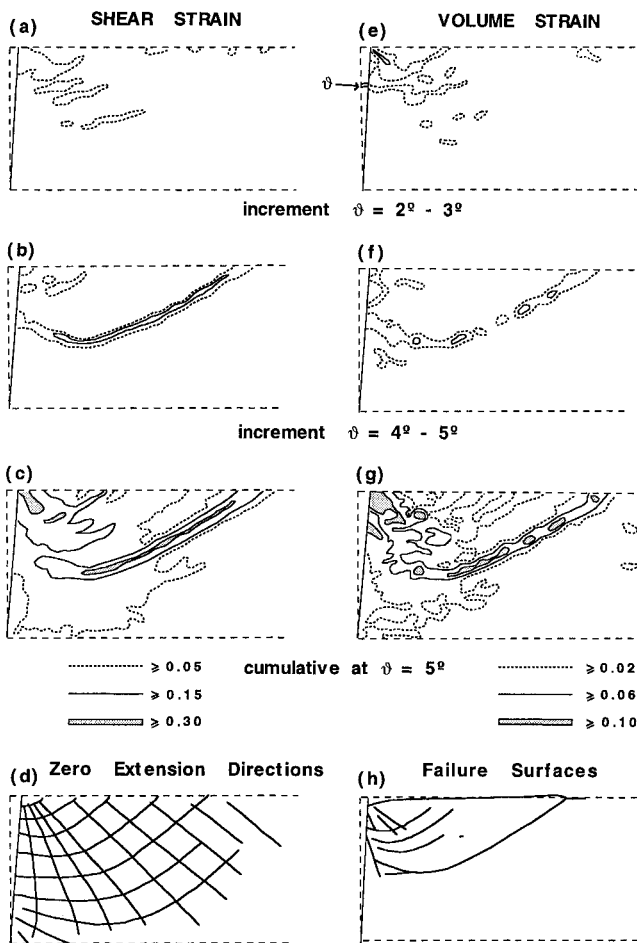


Fig. 4. (a) and (b) Initial outlines of sandbox (broken lines) with contours of incremental shear strains (see key) in sand deformed by rotation, by angle ϑ , of left hand bounding wall of sandbox about bottom left corner. (a) Shear strain increment for rotation from 2 to 3° and (b) increment for rotation from 4 to 5°. (c) Cumulative shear strains at 5° rotation. (d) Zero extension directions at 5° rotation as determined from displacements of lead shot. (e) and (f) Contours of dilatation for the same increments of rotation as in (a) and (b). (g) Cumulative dilatation at 5° rotation. (h) Failure surfaces identified from dark lines on radiograph. Note close correspondence, of both orientations and locations, of incremental and cumulative maximum shear strains and volumetric strains, zero extension directions and failure surfaces. (Redrawn from Roscoe (1970), figs. 21(a–c), 22(e–g), 24(d) and 23(h).)

the principal shortening axis in uniaxial shortening are recorded in the literature on metals (Nadai, 1950), polymers (Bauwens, 1967) and glass (Hagan, 1980). Geological examples are relatively common but of limited value because geological bulk strain, or loading, configurations are usually conjectural, as in the case of the 110° conjugate fractures associated with foliation boudinage (Platt and Vissers, 1980) and the conjugate angles of 109° between regional scale shear zones described by Park (1981). An exceptional case is provided by a pillar of shaley sylvinite at a depth of ca

1000 m in the Boulby mine, Cleveland, UK in which the loading can be assumed to be close to a uniaxial compression. Failure of the pillar is on shear zones with conjugate angles of 109 and 110° (Fig. 3).

3. Dilatational strain

3.1. Failure surface orientations

In a material in which failure is associated with volume strain, dilatation in the case of rocks, the zero extension directions vary from those in the isovolumetric case by an amount determined by the relative amount and sign of the volumetric strain, but the failure plane remains parallel to the zero extension direction. The relationship is well demonstrated in an elegant experiment (Roscoe, 1970) which merits a wider geological audience. Unfortunately, as in so many engineering experiments, the case considered is a special one related to a particular problem rather than a general case. In this experiment the problem addressed was that of failure of a dock retaining wall, a rather specialised example of plane strain. The novel feature of the experiment was that the experimental material, sand, contained a grid of lead shot which allowed measurement of the pre-failure strains which were obtained from a series of radiographs at several stages of deformation.

This experimental design reflected Roscoe's conviction that in order to understand failure, it is necessary first to define and understand the precursory strains, because the location and orientation of a failure surface is defined well before failure or, in conventional terms, well before peak stress. A sand-filled box of rectangular cross-section was confined at one end by a wall hinged at the lower end, simulating the retaining wall. The top of the hinged wall was pushed into the sand until failure occurred (Fig. 4) and radiographs were obtained at successive increments of rotation about the hinge. Contours of incremental and cumulative shear strains, shear strain rates and volumetric strains were produced, together with the trajectories of the principal axes of finite strain, of the zero extension directions and of the failure surfaces as determined by dark lines on the radiographs (Fig. 4). The experiment demonstrated conclusively that the locus of the eventual failure surface was determined by the distributions of precursory shear strains and volumetric strains, the trajectories of which are parallel to one of the two sets of zero extension directions. The zero extension directions are those modified by the dilatation and not those which would occur in a non-dilatant material. Most importantly, the experiment shows that the orientations and locations of major failure surfaces were fixed at an early stage of the deformation, when

both shear and volumetric strains were quite small, and well before a yield surface was developed.

Many experiments have shown that ‘brittle’ failure in rocks is preceded and accompanied by dilatation (e.g. Sano, 1981), but it is nevertheless difficult to quantify the dilatational components of the principal strains. Firstly, it is not known at what stage preceding failure the instantaneous dilatation should be measured. Secondly, although the dilatation is localised, measured volume changes are those of the whole test specimen rather than of the critical region, a problem compounded by volumetric strain gradients within the critical region. The only immediate solution to the problem appears to be ‘reverse engineering’ of an appropriate value for the relative volumetric strain, based on the observed orientations of failure surfaces in experiments. As the most common experimental configuration for rock deformation experiments is uniaxial shortening ($k = 0$), a measure of the relative volumetric strain can be derived from the observed orientations of failure surfaces in these experiments. This value can then be applied to predict failure surface orientations in plane strain, which is assumed to be the bulk strain most commonly associated with faulting.

3.2. Mohr circles and volume strains

Volumetric strains or, as in this case, relative volumetric strains are simply taken account of by using the Mohr construction. Passchier (1991) provides a proof that a Mohr circle for two-dimensional isovolumetric flow is centred on the vertical reference axis and that a Mohr circle centred to the positive side of the reference axis represents dilatant flow. The same principle is used by Bowden and Jukes (1972) to represent three-dimensional strains but their example was restricted to the case of plane strain ($k = 1$). The method is here extended to $k = 0$ strain and can easily be applied to a general strain where k has a value other than 0, 1 or infinity.

For a volumetric strain (Δv) $\epsilon_X + \epsilon_Y + \epsilon_Z = \Delta v$, where Δv is positive for dilatation, and $\Delta v = (v_1 - v_0)/v_0$ where v_0 is the initial volume and v_1 the strained volume. Discussion is limited here to positive volume strains which are small and which can be either elastic or permanent or both. Δv is the product of dilatational extensions along the extended axes (X and Y for a general oblate strain and X for a plane strain or general prolate strain). ϵ_X , for example, comprises a dilatational component and a non-dilatational component, the proportions of which may vary. However, for a general oblate strain the dilatational extensions along the extended axes (X and Y) are in the same ratio as the non-dilatational components of strain on those axes, in accord with St Venant’s Principle (Bowden and Jukes, 1972). For example,

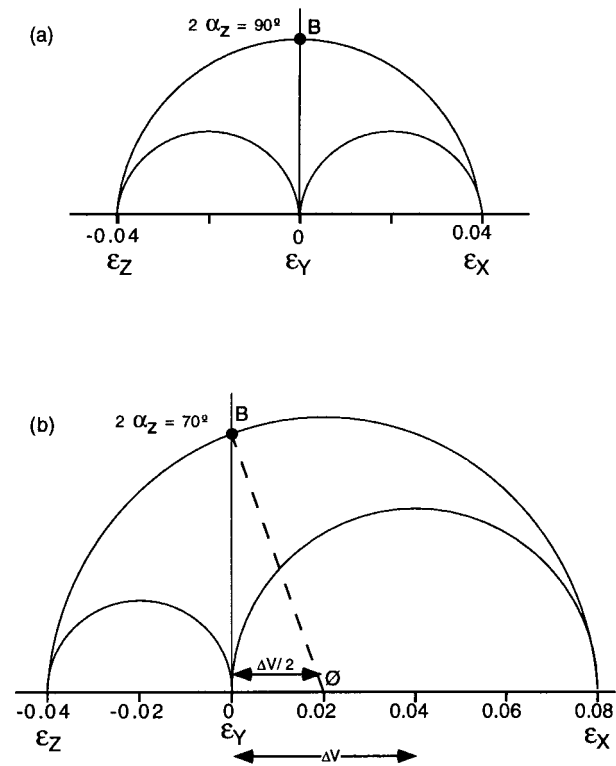


Fig. 5. (a) Mohr representation of constant volume plane strain deformation in matrix and bulk volume, for small strains. Locus of zero extension directions is line OB. (b) Mohr representation of dilatational plane strain deformation in matrix and bulk volume, with centre of the Mohr circle displaced relative to the origin by an amount $\Delta v/2$. The zero extension direction in the XZ plane, point B, is $< 45^\circ$ to Z. OB is the locus of all zero extension lines. O is the original position of the vertical reference axis. The relative amount of dilatational strain is given by the ratio $\Delta v/\epsilon_Z = 1.0$.

with a perfectly oblate strain ($k = 0$) the dilatational components of extensions along the X and Y axes are equal and their product is the volume strain. There is no dilatational component of extension along the principal shortening axis (Z).

For a plane strain, since $\epsilon_Y = 0$, $\epsilon_Z = \Delta v - \epsilon_X$, or $\epsilon_X - \Delta v = \epsilon_Z$, the centre of the Mohr circle is displaced from the vertical reference axis by $\Delta v/2$ (Bowden and Jukes, 1972) parallel to the strain axis (Fig. 5b). The displacement is $\Delta v/2$ because when the diameter of the Mohr circle increases by Δv , by increasing the value of ϵ_X with ϵ_Z remaining fixed, its centre is shifted by $\Delta v/2$. Fig. 5 illustrates two cases of plane strain deformation of a cube with sides of length 10 units, one without volume change (Fig. 5a) and one with an arbitrary amount of dilatation (Fig. 5b). In the isovolumetric case the dimensions of the principal axes of the strained cube are X = 10.4, Y = 10 and Z = 9.6, so $\epsilon_X = 0.04$, $\epsilon_Y = 0$, $\epsilon_Z = -0.04$ and $\epsilon_X + \epsilon_Y + \epsilon_Z = 0 = \Delta v$ (Fig. 5a). With volume strain the dimensions of the principal axes of the strained cube are X = 10.8

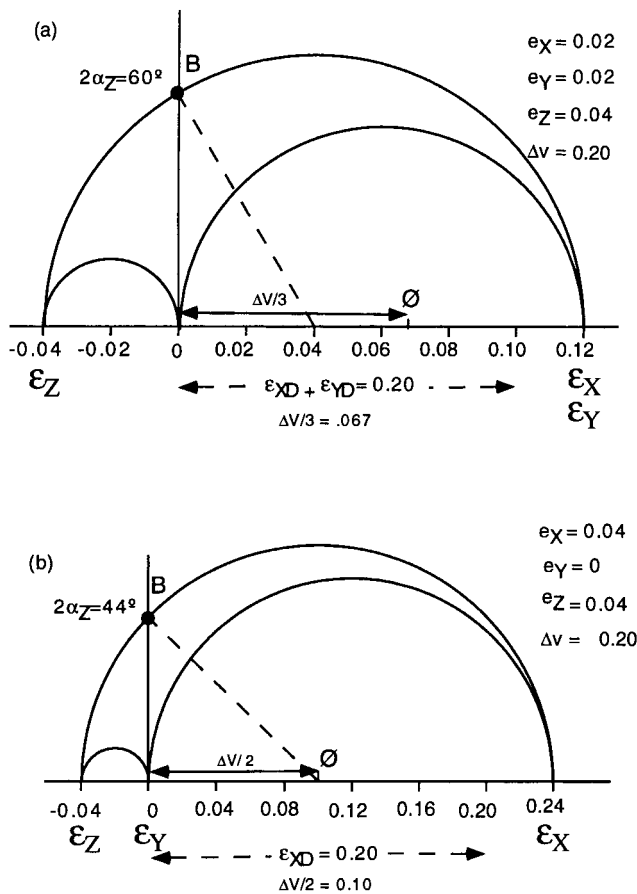


Fig. 6. (a) Mohr circles for uniaxial shortening ($k = 0$) with locus of zero extension directions (OB). Shear fracture (B) at 30° to the Z axis in the plane containing Z, is a typical experimental result which corresponds to a $\Delta v/\epsilon_Z$ ratio of 5.0. ϵ_{XD} and ϵ_{YD} are the dilatational components of ϵ_X and ϵ_Y ($\epsilon_{XD} = \epsilon_{YD} = 0.1$). ϵ_Z and the non-dilatational components of ϵ_X and ϵ_Y are the same as in Fig. 5(b). Ø is the position of the vertical reference axis for isovolumetric uniaxial strain (Fig. 5b). (b) Mohr circles for plane strain ($k = 1.0$) with the same $\Delta v/\epsilon_Z$ (5.0) as in (a), providing a zero extension direction at 22° to Z in the XZ plane ($\epsilon_{XD} = 2.0$ and $\epsilon_{YD} = 0$). ϵ_Z and the non-dilatational components of ϵ_X and ϵ_Y are the same as in Fig. 5(a) and $\Delta v = 2.0$ in both cases. Ø is the position of the vertical reference axis for isovolumetric plane strain (Fig. 5a).

(including dilatational extension of 0.4), $Y = 10$ and $Z = 9.6$, so $\epsilon_X = 0.08$, $\epsilon_Y = 0$ and $\epsilon_Z = -0.04$ and $\epsilon_X + \epsilon_Y + \epsilon_Z = 0.04 = \Delta v$, corresponding to a strained volume of 1040 units (Fig. 5b). Note that the dilatational component of the extension in X is equal to the volume strain. For this particular case in which the dilatational and non-dilatational components of the extension in X are equal, the zero extension direction lies at 35° to the Z axis, compared with 45° for isovolumetric plane strain.

Note that as Δv increases as a proportion of ϵ_X , from the 50% in the case illustrated, the centre of the Mohr circle moves progressively towards Z and the angle between the zero extension direction and the Z

axis decreases, to the limit where $\Delta v = \epsilon_X$ and the zero extension direction is parallel to the Z axis. This limiting case corresponds to the formation of a tension crack. An alternative approach (Roscoe, 1970), which gives the same result, is by reference to the ‘angle of dilation’, w , where

$$(\dot{v}/\dot{\gamma}) = -(\dot{\epsilon}_Z + \dot{\epsilon}_X)/(\dot{\epsilon}_Z - \dot{\epsilon}_X) = \sin w \quad (1)$$

and $(45 - w/2) =$ the angle between the zero strain rate direction and the $\dot{\epsilon}_Z$ axis, $\dot{\gamma}$ = rate of shear strain and strains are expressed as strain rates ($\dot{\epsilon}$).

However, the ‘angle of dilation’ is simply an ad hoc engineering parameter comparable with the ‘angle of internal friction’ in so far as it does not represent an intrinsic material property.

Constant volume and dilatational uniaxial bulk strains ($k = 0$) are illustrated in Fig. 6. Since $\epsilon_X = \epsilon_Y$, $2\epsilon_X + \epsilon_Z = \Delta v$, or $\epsilon_X - \Delta v = \epsilon_Z$, and the centre of the Mohr circle is displaced from the vertical reference axis by $\Delta v/3$ (Fig. 6b). In the isovolumetric case for an initial cube of side 10 units, the dimensions of the principal axes of the strained cube are $X = 10.2$, $Y = 10.2$ and $Z = 9.6$, so $\epsilon_X = 0.02$, $\epsilon_Y = 0.02$, $\epsilon_Z = -0.04$ and $\epsilon_X + \epsilon_Y + \epsilon_Z = 0 = \Delta v$ (Fig. 6a). With volume strain the dimensions of the principal axes of the strained cube are $X = 10.4$ (including dilatational extension of 0.2), $Y = 10.4$ (including dilatational extension of 0.2) and $Z = 9.6$, so $\epsilon_X = 0.04$, $\epsilon_Y = 0.04$ and $\epsilon_Z = -0.04$ and $\epsilon_X + \epsilon_Y + \epsilon_Z = 0.04 = \Delta v$, corresponding to a strained volume of 1040 units (Fig. 6b). Note that the product of the dilatational components of the extensions in X and Y is equal to the volume strain and that the ratios of the dilatational components of extensions in X and Y to their non-dilatational extensional components are the same. The dilatational components of extensions in X and Y are an arbitrary 50% of their total extensions, ϵ_X and ϵ_Y . For this particular case, in which the dilatational and non-dilatational components of the extensions are equal in both X and Y, the zero extension directions lie at 45° to the Z axis, compared with 54.7° for the isovolumetric strain. In this case, as in the plane strain example, $\Delta v - \epsilon_Z = 1.0$ and this ratio is a convenient way of expressing the relative amount of dilatation.

The volumetric strain components of extensions in X ($k \geq 1.0$) or X and Y ($k < 1.0$), when expressed as proportions of the total extensions along these axes, can vary from 0% (isovolumetric strain) to 100% and they determine the zero extension direction and failure surface orientation. Within this range the actual proportion is determined by the material properties and by the confining pressure and must be determined empirically for each case. For this reason it is necessary to use the orientations of failure surfaces to deter-

mine the relative volumetric strains, rather than the converse.

3.3. Experimental data—low confining pressure

Lockner et al. (1992) describe uniaxial shortening experiments on sandstone cylinders at a low confining pressure of 50 MPa. Acoustic emission monitoring demonstrated that events, the products of dilatational cracks, were initially well distributed spatially but became progressively more spatially restricted to define the eventual failure surfaces. The failure surfaces are clearly defined long before failure occurs with significant acoustic emission at 30–40% peak stress. The fracture surfaces, the orientations of which were not restricted by specimen geometry, formed at ca 32° to Z. Many other uniaxial compression experiments on rocks at low confining pressures, together with the shear fracture orientations, are reported in the literature with 30° being a typical value for the angle between the failure surfaces and the Z axis. Without volume change we would expect a failure surface at 54.7° to the X axis (Fig. 5b); a failure surface at 30° is consistent with $\Delta v - \varepsilon_Z = 5.0$ and shift of the Mohr circle with respect to the origin by $\Delta v/3$, with other parameters as shown in Fig. 6(a). Applying the same relative dilatation, i.e. $\Delta v - \varepsilon_Z = 5.0$, to the plane strain case (Fig. 6b) shows a zero extension direction at 22° to the principal shortening axis, consistent with a normal fault dip of 68°. The mean dip of normal faults in British Coal Measures is reported to be 69° (Walsh and Watterson, 1988). The dependence of failure directions on bulk strain configurations means that the ‘angle of internal friction’ of a material varies not only with confining pressure but also with the strain configuration. It is assumed above that, at the same confining pressure and with the same material, all strain configurations will be characterised by the same value of relative dilatancy, $\Delta v - \varepsilon_Z$, but this assumption has not been tested experimentally.

It follows from the above that, for plane strain, angles bisected by the principal shortening axis (Z) between conjugate sets of failure surfaces with normal dip–slip offset should increase with confining pressure, or depth, from ca 44° (dip 68°) at depths of 1–2 km corresponding to the 50 MPa confining pressure of the experiment, to 90° (dip 45°) for plastic yield structures which are likely to predominate at confining pressures greater than ca 300 MPa (see below). Such changes of fault dip with depth are consistent with determinations of fault dips from outcrop and earthquake data, which were also accounted for in terms of failure along zero extension directions by Walsh and Watterson (1988) who also pointed out that normal faults are expected to become vertical at or near the surface. For the common experimental configuration of uniaxial shortening

($k = 0$), we should expect an increase in the conjugate angle containing the Z axis from ca 60° (fault dip 60°) at low confining pressure to 110° (fault dip 35°) at high confining pressure. Angles between these limiting cases will reflect the progressive change from maximum dilatation to isovolumetric failure and the consequent progressive changes in zero extension directions. The quoted 68° for normal fault dips for plane strain bulk deformation at low confining pressure is purely illustrative because the amount of dilatation is material dependent. Results reported by Lockner et al. (1992) indicate that failure in granite is associated with greater relative dilatation than in sandstone at the same confining pressure, i.e. faults in granite will be steeper than those in sandstone at the same depth. Similarly, dips of normal faults will be expected to be shallower in shales than in sandstones because, for the same confining pressure, dilatational strains will be less in shale than in sandstone. Refraction of faults across sandstone–shale boundaries is one manifestation of the difference in dilatancies of these two rock types. The change from rock deformation with volume strain to isovolumetric strain with increase in confining pressure, is illustrated in the two sets of experiments described below.

3.4. Experimental data—high confining pressure

Loading to failure by axial compression of cylinders of Coconino sandstone at a range of confining pressures is described by Friedman and Logan (1973). Failure was primarily by the formation of cataclastic Lüders’ bands with negligible shear displacement. Lüders’ bands are zones of pure shear deformation which may form instead of shear zones when the deformation bands can extend to the boundaries of the deformed volume, but they have the same orientations as simple shear bands. The average conjugate angle between Lüders’ bands increased from 75 to 110° with increase in confining pressure from 35 to 240 MPa. Shear fractures, or macroscopic faults, which also formed in some cases make an angle of 24–35° with the principal shortening axis. In one case, in which the conjugate angle of the Lüders’ bands was 110°, the faults are described as conical rather than planar and thus conform with the conical locus of zero extension directions. Parallel experiments on limestones at confining pressures ranging from 0 to 300 MPa provided Lüders’ bands with conjugate angles increasing from 73 to 103° with increase in confining pressure, and shear fractures with conjugate angles ranging from 37 to 70° although, as the range in a single experiment can be up to 23°, the variation does not correlate with confining pressure.

On the basis of this experimental data fault dips in sandstones, under plane strain conditions, are expected

to decrease with increasing depth from ca 70 to 45° as the dilatation preceding failure decreases to zero.

Particularly revealing are the experiments of Anderson (1974) who investigated kink-band formation by axial compression of cylindrical specimens of slate, with the cleavage parallel to the cylinder axis. Kink-band formation is a typical mode of continuous, and presumably constant volume, shear failure in cleaved rocks and minerals and is equivalent to the formation of plastic yield zones in less anisotropic rocks and materials. In a series of experiments at confining pressures from 0 to 700 MPa, both shear fractures and kink-bands formed at all confining pressures but with shear fractures predominant up to 300 MPa and kink-bands at higher confining pressures. The mean angle between shear fractures and the principal shortening axis was 30.69° (s.d. 6.9°, $n = 129$) in contrast to the mean of 55.4° (s.d. 7.7°, $n = 457$) for kink-bands. For experiments with >5 shear fractures the mean angle between fracture and Z axis increased from 26.1° at 50 MPa ($n = 11$) to 34.4° ($n = 11$) at 400 MPa, as expected from the earlier discussion on variations in proportional dilatation. The dilatations corresponding to these values, when applied to shear fracturing in plane strain deformation, predict normal fault dips of 69° at 50 MPa confining pressure decreasing to dips of 60° at a confining pressure of 400 MPa. The mean angle between fractures and the Z axis in these uniaxial shortening experiments (30.69°), equivalent to a normal fault dip of 69° in plane strain, compares with the values for sandstones of 30° (Friedman and Logan, 1973) and 32° (Lockner et al., 1992). The kink-band conjugate angle of 110.8° is remarkably close to that of 110° reported by Friedman and Logan (1973) for sandstone at their highest confining pressure (240 MPa) and to the theoretical value of 109.8° notwithstanding the possible anisotropy of extensional elastic strains induced by the slaty cleavage in Anderson's experiments. Anderson (1974) also describes structures, referred to as shear zones, intermediate in both deformation mechanism and orientation between faults and kink-bands. The results of Anderson's meticulous experiment, perhaps more than any other data, demonstrate the potential of the zero extension model for the interpretation and understanding of geological shear structures.

4. Discussion

Those with an interest in the history of structural geology will recognise some similarity between what is proposed here and the theory of Becker (1893), who asserted that shear failure occurred parallel to planes of no longitudinal strain which were believed to coincide with circular sections of the (finite) strain ellip-

soid. The belief that failure planes coincide with circular sections of the strain ellipsoid was widely held and applied during the early part of the 20th Century and was still being taught when I was a student in the 1950s. Although Becker's views are now regarded as 'discredited', justifiably so in the case of his misconceptions concerning cleavage, perhaps they deserve more respect than they currently receive because, since his time, zero extension directions have been shown experimentally to coincide with failure planes in a variety of materials. In plane strain the zero extension directions do coincide with circular sections of the strain ellipsoid, although they do not do so with other strain configurations (Treagus, 1986). While the contemporary evidence was against Becker, in so far as normal faults usually dip more steeply than the 45° predicted by his theory, what neither Becker nor his critics took into account is the effect of dilatation on the orientations of zero extension directions; had volume strains been taken into account, Becker's theory could have provided a rationale for the dips of many normal faults.

As the purpose of this short article is to stimulate structural geologists and others to take a fresh look at the potential of strain geometry for providing new insights into heterogeneous yield structures in rocks, the arguments and evidence presented are possibly shorter and more selective than would otherwise be expected. In particular, the congruence between principal strain components in the local strain region, in the matrix and in the bulk volume is referred to only briefly. However, if the concept of failure along zero extension directions is basically sound, as I believe it to be, it can be extended to encompass general strain configurations and, eventually, a quantitative understanding of the energy costs of shear structures of different type and orientation. It is surely axiomatic that the structures we observe are those which most efficiently accommodate the displacements, or forces, imposed on volumes of rock. However, the particular theoretical argument used here for the crucial role of zero extension directions in shear failure is not the only one which could be made. Other lines of argument which might be used include zero extension directions as velocity characteristics (Bransby and Blair-Fish, 1975; Jackson et al., 1992), and an argument based on the accommodation of displacement gradients along shear structures.

Although future progress in developing a failure criterion based on strain might be made by traditional observational methods, it is difficult to see how to overcome the problem that geological bulk strain, or loading, configurations can only be inferred. The same problem applies to stress configurations. As a dedicated non-experimentalist, I see an important role for innovative experiments. Roscoe's insistence (Roscoe, 1970) that attention should be paid to the strains and

structures which precede failure was prescient, so future progress will perhaps emerge from further development of his radiographic technique. Perhaps then we can look forward to a time when strain geometry and kinematics are more generally accepted as the standard tools for interpretation of a variety of geological structures and the philosophical concept of stress is reserved for use only on special occasions.

5. Conclusions

- (i) Failure and yield surfaces in a wide variety of materials have been demonstrated experimentally to form parallel to zero extension directions in a wide range of materials, including rocks.
- (ii) The crucial difference between plastic and 'brittle' failure modes is that the former generally is isovolumetric and the latter is preceded by dilatation.
- (iii) Dilatation changes the orientations of zero extension directions and of the subsequent failure surfaces.
- (iv) The difference in conjugate angles between faults ($<90^\circ$) and plastic shear zones ($\geq 90^\circ$) is a consequence of the dilatation associated with faulting.
- (v) Dips of normal faults are expected to decrease with depth from ca 70° at depths of 1–2 km to 45° at the base of the seismogenic layer.
- (vi) Interpretation of heterogeneous yield structures in rocks in terms of strain geometry and kinematics rather than stresses provides an opportunity for interpreting geological structures in a more unified way than hitherto.

Acknowledgements

Thanks are due to my colleagues in the Liverpool Fault Analysis Group for support and for constructive comments on the manuscript. I am grateful to Chris Talbot for providing the data and sketch for Fig. 3, to Sue Treagus for advice on the Mohr construction and to Richard Lisle and John Cosgrove for helpful reviews which resulted in significant improvement of the manuscript.

References

- Anderson, E.M., 1951. *The Dynamics of Faulting*. Oliver & Boyd, Edinburgh.
- Anderson, T.B., 1974. The relationship between kink-bands and shear fractures in the experimental deformation of slate. *Journal of the Geological Society of London* 130, 367–382.
- Bauwens, J.C., 1967. Yield conditions and propagation of Lüders' lines in tension–torsion experiments on Polyvinyl Chloride. *Journal of Polymer Science* 8 (A-2), 893–901.
- Becker, G.F., 1893. Finite homogeneous strain, flow and rupture of rocks. *Geological Society of America Bulletin* 4, 13–19.
- Bowden, P.B., Jukes, J.A., 1972. The plastic flow of isotropic polymers. *Journal of Materials Science* 7, 52–63.
- Bransby, P.L., Blair-Fish, P.M., 1975. Deformations near rupture surfaces in flowing sand. *Geotechnique* 25, 384–389.
- Burland, J.B., 1965. Deformation of soft clay. PhD thesis, University of Cambridge, UK.
- Edelman, H.S., 1989. Limitations of the concept of stress in structural analysis. *Journal of Geological Education* 37, 102–106.
- Escher, A., Escher, J.C., Watterson, J., 1975. The reorientation of the Kangamiut dike swarm, West Greenland. *Canadian Journal of Earth Science* 12, 158–173.
- Flinn, D., 1962. On folding during three-dimensional progressive deformation. *Journal of the Geological Society of London* 118, 385–433.
- Friedman, M., Logan, J.M., 1973. Lüders' bands in experimentally deformed sandstone and limestone. *Bulletin of the Geological Society of America* 84, 1465–1476.
- Hagan, J.T., 1980. Shear deformation under pyramidal indentations in soda-lime glass. *Journal of Materials Science* 15, 1417–1424.
- Jackson, J., Haines, J., Holt, W., 1992. The horizontal velocity field in the deforming Aegean Sea region determined from the moment tensors of earthquakes. *Journal of Geophysical Research* 97 (B12), 17657–17684.
- Lockner, D.A., Byerlee, J.D., Kuksenko, V., Ponomarev, A., Sidorin, A., 1992. Observations of quasistatic fault growth from acoustic emissions. In: Evans, B., Wong, T.F. (Eds.), *Fault Mechanics and Transport Properties of Rocks*. Academic Press, London, pp. 3–32.
- Nadai, A., 1950. *Theory of Flow and Fracture of Solids*. McGraw-Hill, New York.
- Park, R.G., 1981. Shear-zone deformation and bulk strain in granite–greenstone terrain of the Western Superior Province, Canada. *Precambrian Research* 14, 31–47.
- Passchier, C.W., 1991. The classification of dilatant flow types. *Journal of Structural Geology* 13, 101–104.
- Platt, J.P., Vissers, R.L.M., 1980. Extensional structures in isotropic rocks. *Journal of Structural Geology* 2, 397–410.
- Ramsay, J.G., Graham, R.H., 1970. Strain variation in shear belts. *Canadian Journal of Earth Science* 7, 786–813.
- Ramsay, J.G., Huber, M.I., 1987. *The Techniques of Modern Structural Geology*. In: *Folds and Fractures*, Volume 2. Academic Press, London.
- Roscoe, K.H., 1970. The influence of strains in soil mechanics. *Geotechnique* 20, 129–170.
- Rutter, E.H., 1986. On the nomenclature of mode of failure transitions in rocks. *Tectonophysics* 122, 381–387.
- Sano, M., 1981. Influence of strain rate on dilatancy and strength of Oshima Granite under triaxial compression. *Journal of Geophysical Research* 86 (B10), 9299–9311.
- Taylor, G.I., 1938. Plastic strain in metals. *Journal of the Institute of Metals* 62, 307–324.
- Treagus, S.H., 1983. A theory of finite strain variation through contrasting layers, and its bearing on cleavage refraction. *Journal of Structural Geology* 5, 351–368.
- Treagus, S.H., 1986. Some applications of the Mohr diagram for three-dimensional strain. *Journal of Structural Geology* 8, 819–830.
- Walsh, J., Watterson, J., 1988. Dips of normal faults in British Coal Measures and other sedimentary sequences. *Journal of Structural Geology* 145, 859–873.
- Watterson, J., 1978. Proterozoic intraplate deformation in the light of South-east Asian neotectonics. *Nature* 273 (5664), 636–640.